Polish Journal of Medical Physics and Engineering
The Journal of Polish Society of Medical Physics
ISSN 1898-0309, doi: 10.2478/pjmpe-2023-0014

June 2023
Vol 29, Issue 2

Scientific Paper

Effect of the Small Field of View and Imaging Parameters to Image Quality and Dose Calculation in Adaptive Radiotherapy

Allam UBAIDILLAH[1,BCD], Annisa Rahma FAUZIA[2,B], Adi Teguh PURNOMO[3,BC], Nuruddin NASUTION[2,B], Wahyu Edy WIBOWO[2,BC], Supriyanto Ardjo PAWIRO [1,ABCD,*]

[1]*Department of Physics, Faculty of Mathematics and Natural Sciences, Universitas Indonesia, Depok, West Java, 16424, Indonesia*
[2]*Department of Radiation Oncology, Faculty of Medicine, Universitas Indonesia, dr. Cipto Mangunkusumo General Hospital, Jakarta, 10430, Indonesia*
[3]*PT Elekta Medical Solution, Cowell Tower 7th Floor Unit 2A, Jakarta, 10410, Indonesia*
[*]*Corresponding author: Dr. Supriyanto Ardjo Pawiro; supriyanto.p@sci.ui.ac.id*

(received 14 April 2023; revised 8 June 2023; accepted 12 June 2023)

Abstract

Background: The use of cone beam computed tomography (CBCT) for dose calculation in adaptive radiotherapy has been investigated in many studies. Proper acquisition and reconstruction of preset parameters could improve the accuracy of dose calculation based on CBCT images. This study evaluated the impact of the modified image acquisition and preset reconstruction parameter available in X-Ray Volumetric Imaging (XVI) to improve CBCT image quality and dose calculation accuracy.

Materials and methods: Calibration curves were generated by scanning the CIRS phantom using CBCT XVI Elekta 5.0.4 and Computed Tomography (CT) Simulator Somatom, which served as CT image reference. Rando and Catphan 503 phantoms were scanned with various acquisition and reconstruction parameters for dose accuracy and image quality tests. The image quality test is uniformity, low contrast visibility, spatial resolution, and geometrical scale test for each image by following the XVI image quality test module.

Results: Acquisition and reconstruction parameters have an impact on the Hounsfield Unit (HU) value that is used as the HU-Relative Electron Density (RED) calibration curve. The dose difference for all the calibration curves was within 1% and passed the gamma passing rate. Images acquired using 120 kVp, F1 (with Bowtie Filter), and 50 mA (F1-120-50-10) scored the highest Gamma Index (GI) of 98.5%. For the image quality test, it scored 1.20% on the uniformity test, 2.14% on the low contrast visibility test, and 11 lp/cm on the spatial resolution test. However, F1-120-50-10 reconstructed with different reconstructions scored 3.83% and 4 lp/cm in contrast and spatial resolution test, respectively.

Conclusion: CBCT reconstruction parameters work as a scatter correction. It could improve the dose accuracy and image quality. Nevertheless, without adequate CBCT acquisition protocols, it would produce an image with high uncertainty and cannot be fixed with reconstruction protocols. The F1-120-50-10 protocols generate the highest dose accuracy and image quality.

Keywords: radiotherapy; adaptive radiotherapy; calibration curve; cone beam computed tomography.

Introduction

Adaptive radiotherapy (ART) aims to consider the changes in the patient's anatomy during radiation treatment.[1–3] These changes might be visible through the CBCT system during patient position verification.[2] Based on these changes, patients could then undergo rescan using CT Simulator. ART is usually done using CT simulator images once the patient's anatomy changes have been identified, commonly using the CBCT system. Thus, the dose calculation could be more optimized.[4-6] Same as CT Simulator, CBCT also contain voxels which are able to acquire the knowledge needed in dose calculation. Because of that, the CBCT images have a potential to be used for dose calculations just like CT images.[7-9] The knowledge needed in dose calculation are calibration curve which then will be used in treatment planning system (TPS), that can be obtained through voxels in the image receptors.[6,7,10] Despite being able to obtain the information needed in dose calculation, there are several challenges for using the CBCT images in dose calculation.

The following challenges come from the Hounsfield Unit (HU) in CBCT images that rely on many parameters such as tube voltage, filters, electric current (mAs), and reconstruction algorithm, just like in CT Simulator.[11-13] However, CBCT uses

© 2023 Authors This is an open access article licensed under the Creative Commons Attribution-NonCommercial-NoDerivs License (http://creativecommons.org/licenses/by-nc-nd/4.0/).

Authors' contribution: A – Research concept and design, B – Collection and/or assembly of data, C – Data analysis and interpretation, D – Writing the article, E – Critical revision of the article, F – Final approval of the article.

a conical geometry beam and a flat panel detector to obtain the entire patient volume during a single linac rotation.[12,14-16] This mechanism is more prone to additional artefacts, such as scatter and noise which are caused by the beam divergence.[17] The way CBCT acquire its images is by reconstructing two-dimensional (2D) X-ray projections acquired in a circular orbit around the target object into a volume.[17] Although, using only a single circular orbit is not enough for an accurate reconstruction of the entire volume.[17] Nevertheless, this acquisition mechanism is faster than CT simulator and suitable for patient position verification.[4,14] Another challenge comes from the image quality of CBCT images itself. The further away from the isocentre, the image quality will degrade, which is a problem in high Field of View (FOV) images.[17] Even so, previous studies have shown that CBCT images are capable of being used in dose calculation.[13,18]

In dose calculation, the difference in Hounsfield Unit between CBCT and CT simulator images is bound to happen. There have been several attempts to decrease this difference in previous studies, for instance by subtracting the images using ImageJ Software (National Institutes of Health).[13,18] If the difference is more than 100 HU, it could lead to a dose calculation error of up to 2%.[13] Consequently, it is necessary to use a suitable CBCT pre-set that produces an appropriate calibration curve.

The main focus is the imaging parameter in a small mode field of view which is available on CBCT XVI (Elekta Oncology Systems, UK), mainly used for head and neck (HN) radiation treatment. Smaller FOV results in smaller noise and artefacts which makes it easier to study in a short amount of time. By evaluating various pre-set and its effect, in the end, a pre-set that could generate an optimal output could be yielded.

Materials and Methods

Materials

This work was conducted using X-ray Volumetric Imaging Cone Beam Computed Tomography Elekta 5.0.4, CT Simulator Somatom, CIRS 062MA Phantom, Rando Phantom, Catphan 503 Phantom, TPS Monaco 6.0.0, and PTW Verisoft.

The CBCT XVI Elekta system is mounted on the gantry of Elekta Versa® (Elekta, Stockholm, Sweden). CBCT XVI could acquire volumetric images using three different FOVs that depend on the acquisition protocol: Small (S) (27 cm), Medium (M) (41 cm), and Large (L) (52 cm). For each FOV, there are additional collimators marked 10, 15, and 20 in the form of cassettes which could be inserted into the XVI outlet. Other cassettes that represent a bowtie filter is called F1 and F0 to represent its absence.[8,18-20] By scanning the electron density (ED) CIRS phantom (CIRS Model 062MA, CIRS Tissue Simulation Technology, Norfolk, USA) using diverse acquisition and reconstruction parameters, a measurement of the 3D (3-Dimension) CT Value could be done. CIRS phantom had a width of 330 mm, length of 250 mm, height of 270 mm and various plugs that contain varied densities that are shown in **Table 1**; each plug has a diameter of 3 cm and length of 5 cm. Using these mixed densities, it could generate a calibration curve Hounsfield Unit – Relative Electron Densities (HU-RED) which were used in dose calculation. For the dose calculation, the phantom used was the head of Rando Phantom since it has a human-like structure to study the impact of different pre-set. Rando Phantom is divided into 35 separate slices with a thickness of 2.5 cm.[13] Another phantom also used is Catphan 503 phantom to evaluate the CBCT image quality. Catphan phantom contains several modules which are used to measure various image quality tests; it has a diameter of 15 cm.

Table 1. Relative ED for each of the CIRS phantom inserts

Material	Relative ED
Lung (Inhale)	0.2
Lung (Exhale)	0.496
Adipose	0.949
Breast	0.976
Muscle	1.043
Liver	1.052
Bone 200 mg/cc	1.117
Bone 800 mg/cc	1.456

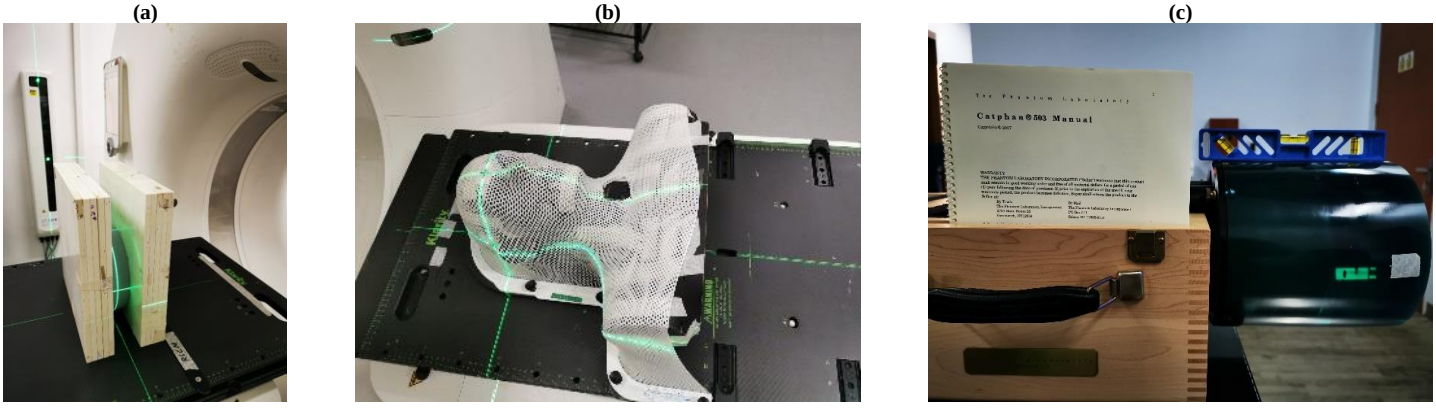

Figure 1. Phantoms used in this study: (a) CIRS, (b) Rando Anderson, and (c) Catphan 503 Phantom

Image Acquisition

Phantom images were acquired using CT Simulator as an image reference and CBCT XVI using the parameter described in **Table 2** and **Table 3** for HN location. In a previous study, the S20 collimator generated the most comparable dose calculation to the CT Simulator dose calculation.[13] Hence, by exploring various acquisition and reconstruction parameters using S20 FOV, the most optimal pre-set protocols could be found. Scanning using S20 FOV moves the gantry by 200° or half-scan. This happens because S20 FOV was positioned at the centre of the X-ray beam with respect to the flat-panel detector.[13]

Obtaining the CIRS phantom images with S20 FOV uses the inner head insert that has a diameter of 180 mm placed in between two 5 cm thick water equivalent slabs. This is done in order to simulate actual patient conditions by introducing additional scatter.[13,21] After generating CIRS images, the resulting calibration curve was used in dose calculation. Dose calculation requires the images of the head and neck of the Rando Phantom. A mask was also used in order to minimize any unnecessary movement. Three markers were placed on top of the mask on the left, centre, and right side of the head phantom. Both CIRS and Rando phantom are shown in **Figure 1a** and **Figure 1b**. The last phantom scanned is the Catphan 503 phantom shown in **Figure 1c**, which was scanned according to the XVI image quality test module.

Image Reconstruction

After the acquisition process, the data must undergo a reconstruction process to form a volumetric data set. Data reconstruction depends on acquisition parameters (voxel size, FOV, number of projections), hardware (processing speed, data output from acquisition computer), and software (reconstruction algorithm) used. Reconstruction should be completed in less than 3 minutes to suit clinical needs.[22]

In XVI CBCT systems, there are specific reconstruction parameters that can be changed. Each parameter has its particular function, and changing it might affect the algorithm. Thus, the outcome might be different. The algorithm could turn the quality higher, longer reconstruction time, and vice versa. There are two reconstruction parameters provided by the XVI, namely: Medium Resolution (MR) and High Resolution (HR). Both are different in terms of their reconstruction voxel size; HR has a smaller voxel size and more image slices resulting in a higher quality of images. MR protocols are commonly used in clinical practice due to their faster reconstruction time. It only takes less than 1 minute, while HR protocols could take up to 2 minutes.[11,23]

Table 2. Irradiation parameters related to the CT Simulator acquisition protocols

Irradiation parameters	Value
Tube Voltage (kVp)	120
Effective mAs	560
Slice Thickness (mm)	5
FOV (mm)	312

Table 3. Irradiation parameters related to the CBCT acquisition protocols

Irradiation parameters	Value
Collimator	S20
kVp	100; 120
(mA, ms/frame)	(10,10); (20,10); (40,10); (50,10); (80,10)
(Total mAs)	(36.1); (72.2); (144.4); (180.5); (288.8)
Filter	F0; F1
Frame	361

Table 4. Reconstruction parameters related to CBCT reconstruction protocols

Reconstruction Parameters	HR	MR	SR	IQ
ReconstructionVoxelSize	0.5	1	0.5	0.5
ReconstructionDimensionX	540	270	540	540
ReconstructionDimensionY	520	264	520	64 or 520*
ReconstructionDimensionZ	540	270	540	540
ReconstructionOffsetX	0	0	0	0
ReconstructionOffsetY	0	0	0	0
ReconstructionOffsetZ	0	0	0	0
ReconstructionFilter	Wiener	Wiener	Wiener	Wiener
NumberOfReconstructionFilterParameters	2	2	2	2
ReconstructionFilterParameter1	0.05	0.05	0.05	0.05
ReconstructionFilterParameter2	90	90	10	90
Interpolation	Partial2	Partial2	Bilinear	Partial2
ScatterCorrection	Uniform	Uniform	Uniform	Uniform
NumberOfScatterCorrectionParameters	1	1	1	1
ScatterCorrectionParameter	0.24	0.24	0.24	0.24
ReconstructionDataType	Float	Float	Short	Short
PreFilter	None	None	Median5	None
ProjectionDownSizeFactor	1	2	1	2 or 1**

**For geometric test; **For spatial resolution test*

Investigation of the reconstruction process was done using three types of reconstruction: Medium (M), High (H), Image Quality reconstruction (IQ), and research reconstruction (S), as shown in **Table 4**.[21] The S-reconstruction is an alteration of XVI H-reconstruction, by changing certain parameters. Higher-quality images could then be produced. The "ReconstructionFilterParameter" was changed from 90 to 10 since it affects the noise or spatial frequency distribution from the image reconstructed. The "Interpolation" algorithm that controls the back projection was changed from "Partial2" to "Bilinear", which could produce better reconstruction output, but it takes a longer time. The "ReconstructionDataType" was changed from "Float" to "Short" because it could develop a faster reconstruction time at the cost of lower-quality image output. The last parameter is "PreFilter", which controls contrast and resolution. It was changed from "None" to "Median5", which produces a lower resolution but higher contrast. This reconstruction could take up to 5 minutes.

Calibration Curve

After acquiring the images from CT and CBCT, all of the images were imported into Monaco TPS version 6.1.1. The measurement of mean HU values was done by making a circle Region of Interest (ROI) with a diameter of 160 mm for all inserted materials.[13,18] Next, the mean HU values acquired were compared between CBCT and CT images for each image generated by each acquisition.[13,18] By subtracting it, which of CBCT acquisition protocols could generate mean HU with the slightest difference, or no more than 100 HU from the CT image.[13]

The study chose two acquisition protocols with the lowest mean HU difference and plotted the mean HU value as a function of RED given by phantom manufacturers in **Table 3**. In order to be able to see the effect of acquisition parameters, the study also plots a calibration curve using acquisition protocols which XVI recommends. In order to see the effect of reconstruction parameters, the study also plotted calibration curves on the same images but with different reconstruction parameters.

Contouring and Image Registration

The CBCT Rando images were produced using three different acquisition and reconstruction protocols. In the end, there were ten images (1 CT and 9 CBCT images) that would be used. The Rando images were imported into Monaco TPS for contouring and dose calculation. The contouring process, shown in **Figure 2**, is first done on Rando CT images using Task Group 119 (TG 119)[24] contour for Head and Neck, then adjusting its position according to the correct anatomical position.[25] Using image registration, contour from CT images can be copied into CBCT images. The existence of a marker and each slice were made the same sizes to facilitate the image registration process.[24]

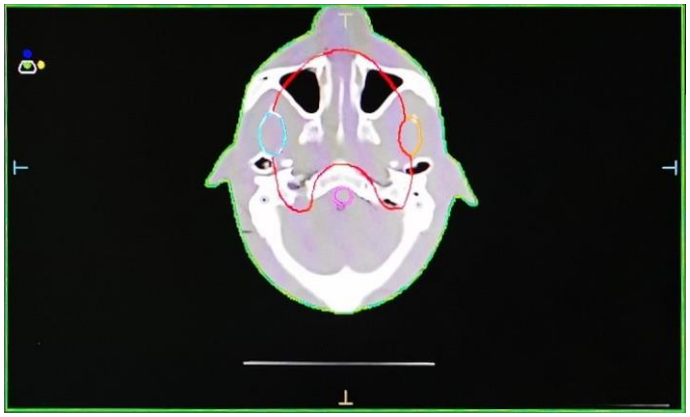

Figure 2. Contouring process using CT Simulator images based on TG 119

Dose Calculation and Evaluation

The dose calculation process with Intensity Modulated Radiotherapy (IMRT) technique used 6 MV and nine fields in an interval of 40°, and for Volumetric Modulated Arc Therapy (VMAT) technique, two complete complementary arcs were used. The beam arrangement is shown in **Figure 3a** and **Figure 3b**.[24,26] Rando phantom consists of several slices that can move during the scanning process with different modalities. In order to minimize the dose calculation uncertainty, Rando phantom images were positioned with a mask to ensure no movement happens during image acquisitions. Different protocols obtained the images using different voxel sizes.

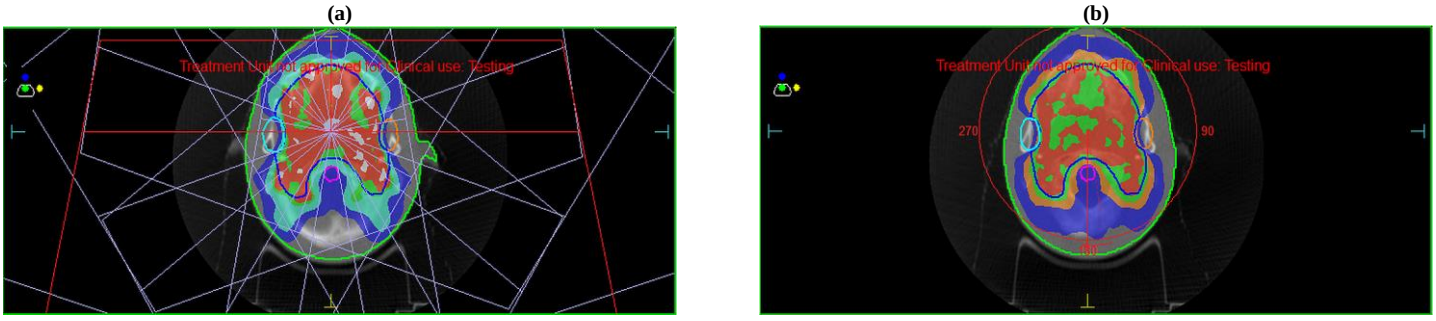

Figure 3. Planning process using F0-100-10-10 images (a) IMRT Technique and (b) VMAT Technique

Hence, all image slices were equalized into 5 mm. For dose calculation, the first process was done on CT images and optimized in the treatment planning system Monaco. After dose goals were achieved, the treatment planning was saved into a template. Planning on CBCT images uses the same plan template while assigning the correct calibration curve for each Rando CBCT image. Dose calculation using the same template could be done without re-optimizing. This process ensures that the CT and CBCT images are identical; the only difference between them is their calibration curve.

Evaluation of the dose distribution uses Conformity Index (CI) and Homogeneity Index (HI). The conformity Index is a region in Planning Target Volume (PTV) covered wholly by Treated Volume in which the Treated Volume (TV) is a tissue volume that receives the prescribed dose, it shows how conformal the dose distribution is.[27] CI formula in Monaco Treatment Planning System (TPS) uses this equation:

$$CI = \frac{(V_{Rx})^2}{(TV \times V_{RI})} \quad \text{Eq. 1}$$

where TV is the structure volume, V_{Rx} is the structure volume covered by the dose of interest, and VRI is the total volume of the dose of interest. According to Monaco TPS, this conformity index describes the degree to which the prescribed isodose volume conforms to the shape and size of the target volume. Meanwhile, the Homogeneity Index (HI) shows how homogeneous the dose distribution is to the target volume. Mathematically HI can be found using this equation:

$$HI = \frac{D_{2\%} - D_{98\%}}{D_{50\%}} \quad \text{Eq. 2}$$

Other method is by comparing all the 3D dose distribution using the 3D gamma index method with Verisoft Software (PTW Freiburg, Germany) using 2%/2 mm Dose Difference (DD) and Distance to Agreement (DTA) criteria. In addition, the dose to the PTV and Organ at Risk (OARs) were compared using the Dose Volume Histogram (DVH) (D20%, D90% and D98%). comparing the DVH would be using Friedman statistical method to find the significance difference among each DVH calculated using different calibration curve.

Image Quality

The image quality test was done in order to find an optimal acquisition and reconstruction protocols that can result an image with optimal image quality and could generate an accurate dose calculation. The tests carried out were uniformity test, low contrast visibility test, spatial resolution test, and scale test. Each test will be done using the same chosen acquisition protocols to see its impact towards the quality of an image. These three tests can determine the image's ability to differentiate each object, especially objects with similar density.

Uniformity tests require the mean value of each location with the same distance of 4.5 cm within the Catphan phantom module. Besides that, this test requires the mean value from the isocentre. This test has a tolerance of 1.5%. After acquiring the mean value from each location, the maximum and minimum mean values are used to find the difference using this equation:

$$Uniformity = \left(\frac{mean(high) - mean\ (low)}{mean(high)}\right) \times 100\% \quad \text{Eq. 3}$$

The low contrast visibility test needs mean value and standard deviation for polystyrene and Low-Density Polyethylene (LDPE) inserts. Both mean values will be used to find the image's capability to differ between different densities. The equation that could be used is:

$$Low\ Contrast\ Visibility = \left(\frac{\frac{CT_{polystyrene} - CT_{LDPE}}{10}}{\frac{mean_{polystyrene} - mean_{LDPE}}{(SD_{polysterene} + SD_{LDPE})/2}}\right) \times 100\% \quad \text{Eq. 4}$$

The spatial resolution only needs to count the number of pairs of lines that can be seen. This test has a minimum of 10 lp/cm. The scale test is performed in vertical, horizontal, and sagittal directions. The scale test has to calculate the distance between Delrin and LDPE inserts, the distance between two air inserts, and the distance between module 1 and module 4. The vertical and horizontal test have tolerance of 117 ± 1 mm, and the sagittal test have a tolerance of 110 ± 1 mm.

Results

HU-RED Calibration Curve

Figure 4 shows the HU-RED Calibration curve from all of the acquisition protocols, **Figures 4a** and **4b** show several acquisition protocols using 100 kVp with F0 and F1, while **Figure 4c** and **4d** show acquisition protocols using 120 kVp with F0 and F1. Using higher mAs could improve the HU value, this happens to all of the protocols for 100 kVp or 120 kVp. While applying 120 kVp, the presence of a filter results in similar results to when a filter is not used. An increase of HU value is spotted when using mAs higher than 180.5 mAs (50 mA and 10 ms) with 120 kVp and F1, despite that the difference of HU value for all inserts are still below 100 HU.

The protocol with F1, 80 mA and 50 mA, along with 120 kVp, generates the lowest mean HU difference for each insert when compared to CT. These parameters will be written as F1-120-80-10 and F1-120-50-10 because it uses 80 or 50 mA and 10 ms per frame. For comparison, the XVI recommendation protocols that use F0 with 10 mA, 10 ms and 100 kVp were also chosen. This protocol has a difference in mean HU value of 153 HU for water inserts and 352 for bone 800 mg/cc inserts. This parameter will be written as F0-100-10-10 because it uses 10 mA and 10 ms per frame. The CBCT with F1 indicate an improvement of mean HU value since it reduces the dynamic range demanded by the detector. Bowtie Filter also has an effect on reducing scatter, improving beam hardening, and decreasing artefacts.

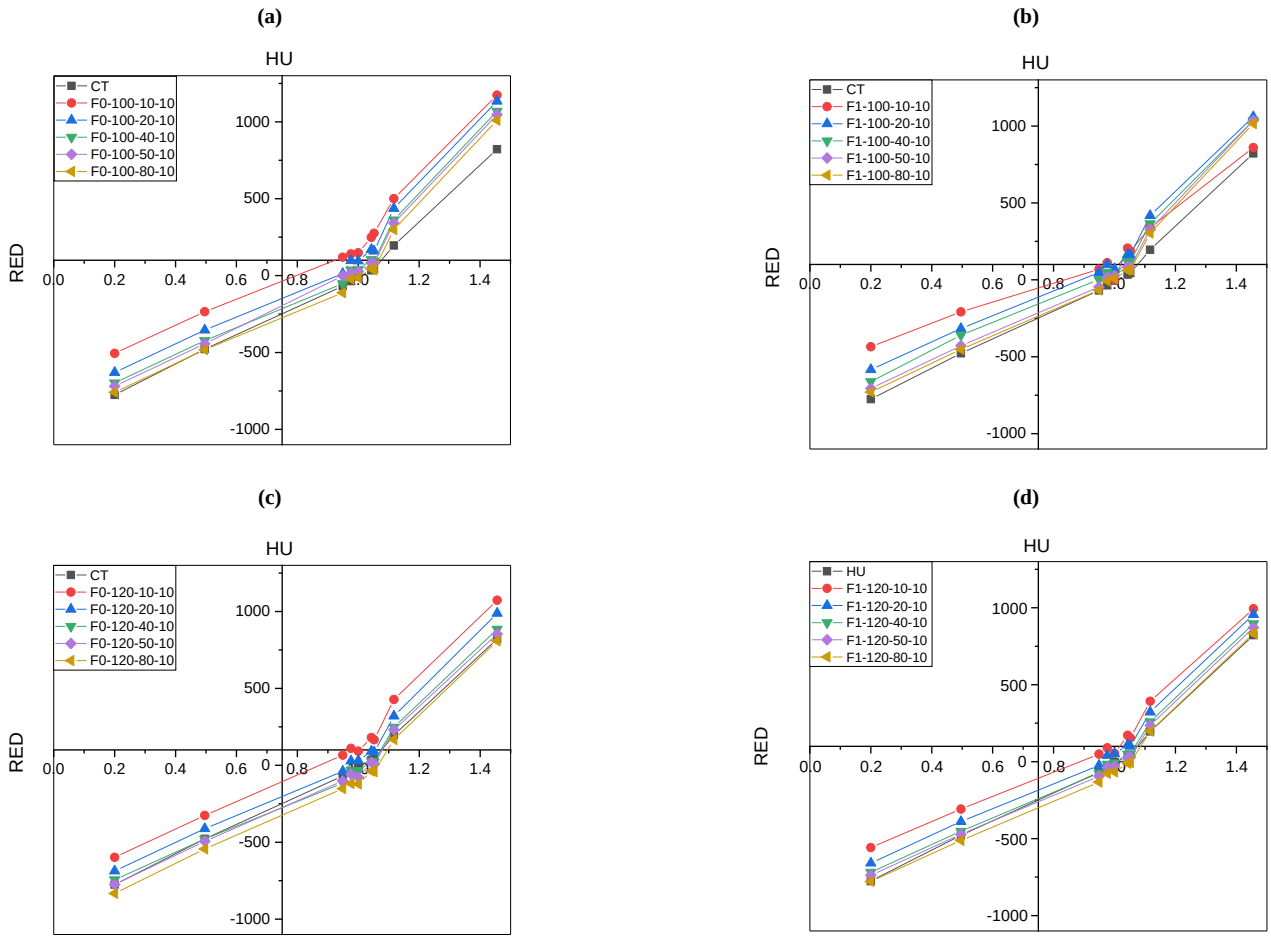

Figure 4. HU-RED calibration curves with (a) 100 kVp and F0, (b) with 100 kVp and F1, (c) 120 kVp and F0, and (d) 120 kVp and F1

Figure 5 shows the HU-RED calibration curve for F1-120-80-10, F1-120-50-10, and F0-100-10-10, while **Tables 5** to **7** show the difference of different reconstruction protocols. The CBCT reconstruction algorithm also works as a scatter correction. Different reconstruction result in nonidentical images, which are visible in **Figure 6**. Other than that, different reconstruction has different HU value, and S-reconstruction tend to have a smaller HU value difference when compared to CT Image. The F0-100-10-10 protocols reconstructed using three kinds of reconstruction protocols do not have a single insert that has a difference of less than 100 HU. Despite that, all reconstructions for F1-120-80-10 and F1-120-50-10 have a HU value no higher than 100 HU.

Table 5. Mean HU value difference using different reconstruction

Material	CT	F1-120-50-10-S	F1-120-50-10-M	F1-120-50-10-H
		Δ	Δ	Δ
Lung Inhale	-776	38	80	83
Lung Exhale	-478	6	50	49
Adipose	-69	-26	14	15
Breast 50/50	-36	-2	37	36
Water	-5	-25	13	13
Muscle	34	-8	33	30
Liver	43	-13	28	24
Bone 200mg/cc	196	40	77	76
Bone 800mg/cc	822	49	83	77

Table 6. Mean HU value difference using different reconstruction

Material	CT	F1-120-80-10-S	F1-120-80-10-M	F1-120-80-10-H
		Δ	Δ	Δ
Lung Inhale	-776	-2	42	41
Lung Exhale	-478	-34	-18	10
Adiposa	-69	-64	-25	-24
Breast 50/50	-36	-40	-2	-3
Water	-5	-62	-24	-25
Muscle	34	-45	-7	-7
Liver	43	-49	-11	-10
Bone 200mg/cc	196	2	38	36
Bone 800mg/cc	822	11	41	44

Table 7. Mean HU value difference using different reconstruction

Material	CT	F0-100-10-10-S	F0-100-10-10-M	F0-100-10-10-H
		Δ	Δ	Δ
Lung Inhale	-776	270	292	306
Lung Exhale	-478	243	268	270
Adipose	-69	189	219	204
Breast 50/50	-36	177	237	224
Water	-5	153	181	158
Muscle	34	215	243	221
Liver	43	232	221	207
Bone 200mg/cc	196	305	328	303
Bone 800mg/cc	822	352	390	307

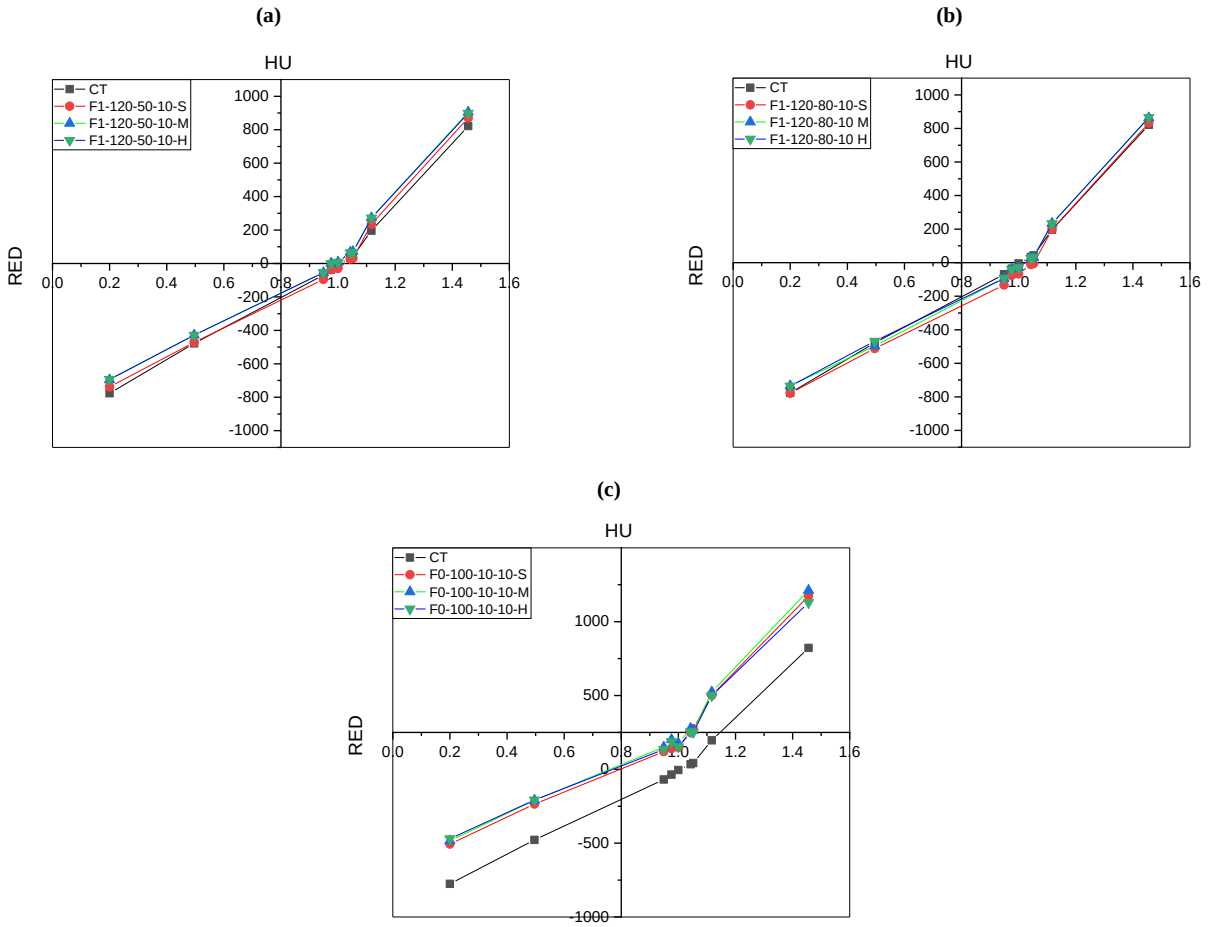

Figure 5. HU-RED Calibration curve using different reconstruction for (a) F1-120-50-10; (b) F1-120-80-10; and (c) F0-100-10-10 used in dose calculation

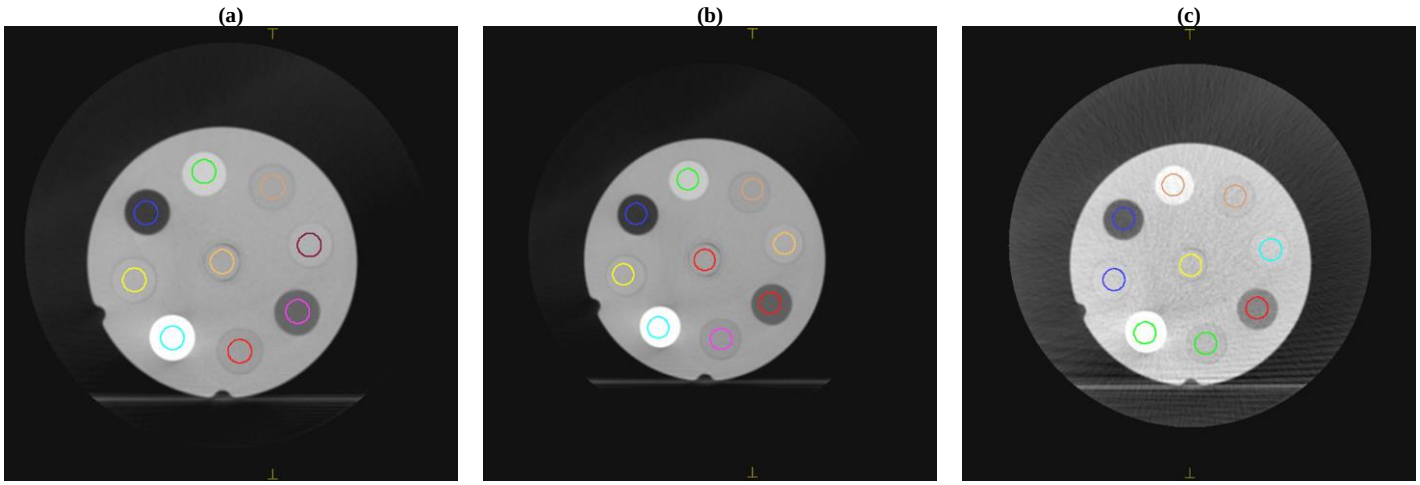

Figure 6. CIRS phantom photograph using (a) F1-120-50-10; (b) F1-120-80-10; and (c) F0-100-10-10 acquisitions protocols

Dose Calculations

All of the percentage differences are shown in **Figure 7** for F0-100-10-10 only passed the criteria once. It happens for the IMRT technique using the XVI Medium reconstruction parameters. The other acquisition parameters can meet all of the dose criteria. The highest difference in PTVs when using IMRT techniques is 1.29% from F1-120-180.5 using XVI Medium reconstruction parameters, while using VMAT techniques is 0.58% from F0-100-10-10 using our reconstruction parameters.

Table 8 shows the information about CI and HI using D2%, D50% and D98%. For HI, the closer its value to zero means, the more homogenous its dose distribution. The lowest value is 0.072 and 0.089 for VMAT and IMRT techniques, respectively. Meanwhile, for CI, the closer its value to one means, the more conformal dose distribution is. The highest value is 0.93 and 0.86 for VMAT and IMRT techniques, respectively. However, the maximum dose (D_{max}) difference between CT and CBCT for OARs is almost as high as 3.5%.

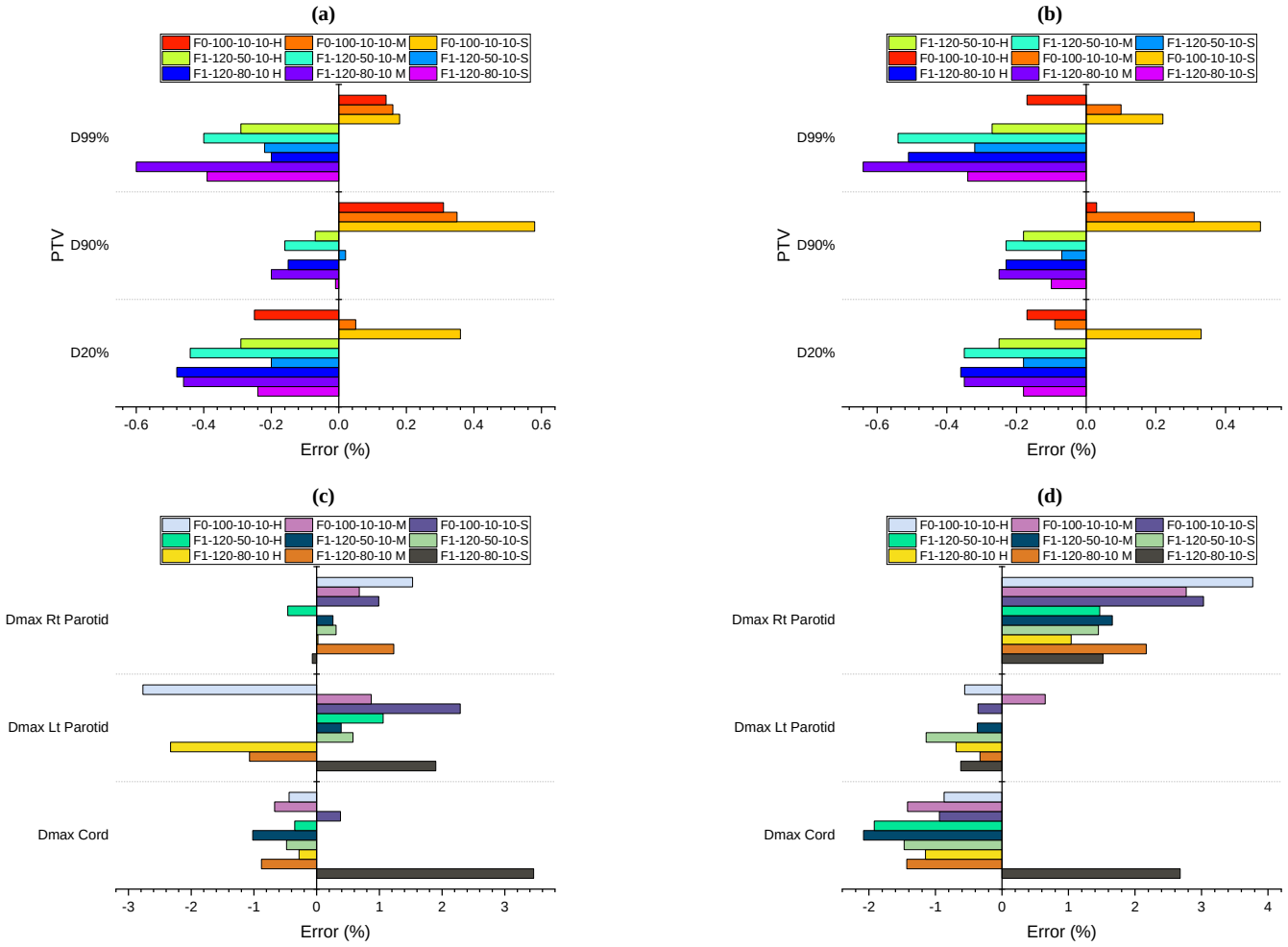

Figure 7. Percentage dose difference of PTV and OARs (a) PTV in IMRT techniques, (b) PTV in VMAT techniques, (c) OARs in IMRT techniques, and (d) OARs in VMAT techniques calculated using different calibration curves of CT and CBCT

Table 8. Conformity, Homogeneity, and Gamma Index

Acquisition Protocols	VMAT					IMRT				
	CI	Δ(%)	HI	Δ(%)	GI	CI	Δ(%)	HI	Δ(%)	GI
CT	0.92	-	0.072	-	-	0.85	-	0.090	-	-
F1-120-80-10-S	0.91	1.09	0.072	-0.46	98.2	0.85	0	0.089	1.15	98.3
F1-120-80-10-M	0.93	-1.09	0.074	-3.25	98.0	0.86	-1.18	0.090	0.04	97.6
F1-120-80-10-H	0.93	-1.09	0.076	-6.04	98.1	0.86	-1.18	0.091	-1.07	97.8
F1-120-50-10-S	0.86	6.52	0.073	-1.85	98.3	0.83	2.35	0.090	0.04	98.5
F1-120-50-10-M	0.92	0	0.075	-4.64	97.8	0.86	-1.18	0.090	0.04	98
F1-120-50-10-H	0.91	1.09	0.073	-1.85	98.1	0.84	1.18	0.091	-1.07	98.4
F0-100-10-10-S	0.88	4.35	0.074	-3.25	97.6	0.84	1.18	0.089	1.15	97.9
F0-100-10-10-M	0.89	4.35	0.074	-3.25	97.9	0.86	1.18	0.092	-2.18	98
F0-100-10-10-H	0.89	3.26	0.080	-11.62	96.8	0.86	-1.18	0.094	-4.4	97

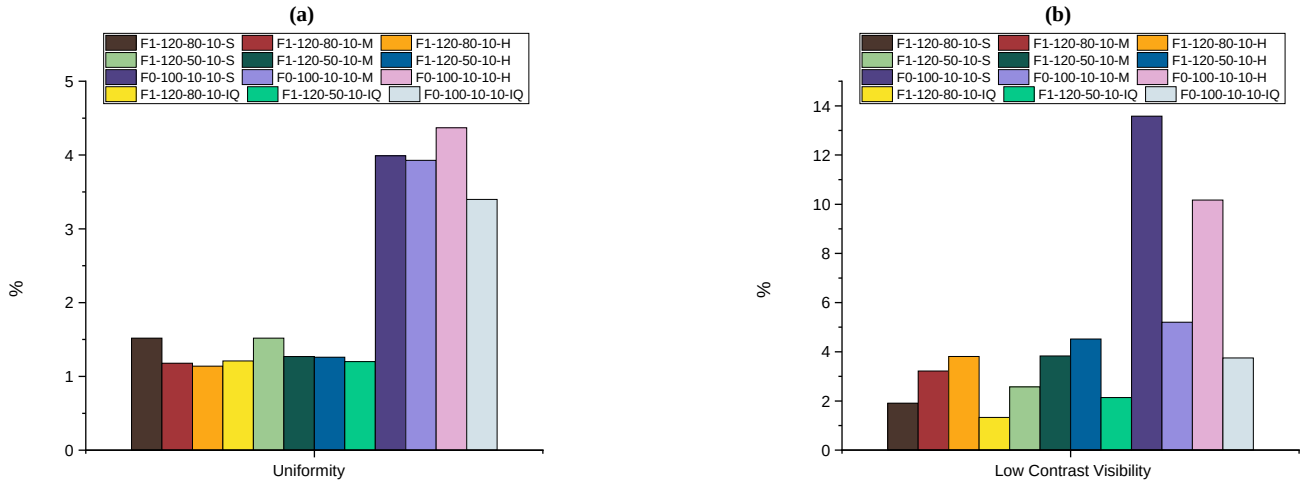

Figure 8. Results of (a) Uniformity test, and (b) Low Contrast Visibility test

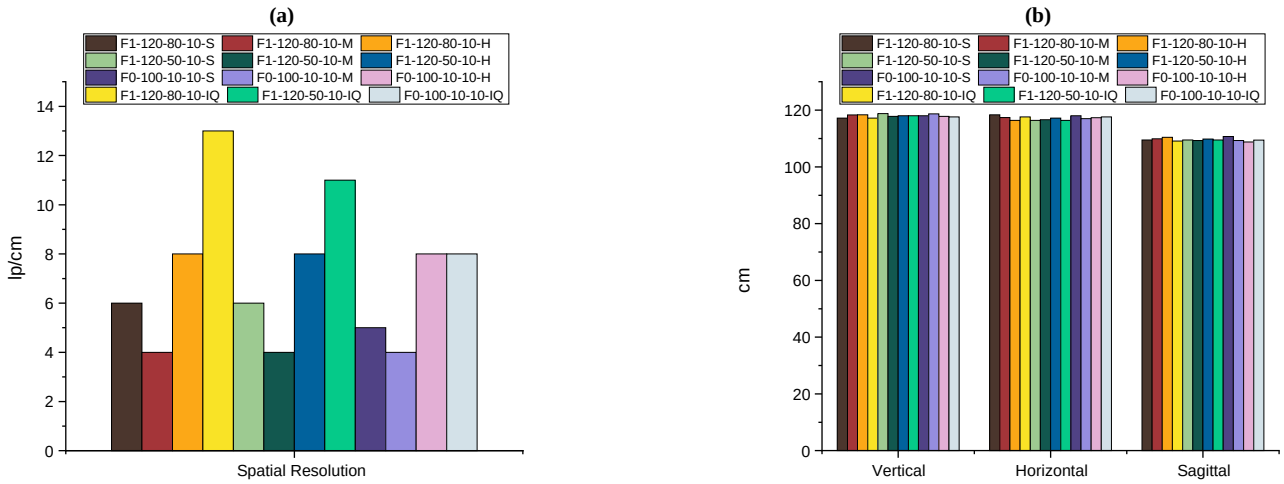

Figure 9. Results of (a) Spatial Resolution test, and (b) Transversal and Sagittal scale test

Dose Distribution Comparison

The results obtained from the 3D gamma index (GI) are shown in **Table 8**. With gamma criterion DD/DTA 2%/2 mm. It shows a good correspondence between the dose distribution of CT images and CBCT images. The lowest GI happens when comparing CT dose distribution with F0-100-10-10-M with the VMAT technique it is 96.8%. The highest value happens when comparing CT dose distribution with F0-120-50-10 with the IMRT technique, which is 98.5%.

Image Quality Test

Figure 8a shows the results of uniformity. The highest uniformity test score is 4.37% for F0-100-10-10 using H-reconstruction. The same protocol using IQ-reconstruction is 3.4%, which is also higher than the minimum tolerance of 1.5%. The F1-120-50-10 and F1-120-80-10 yield 1.2% and 1.21% using IQ-reconstruction and 1.52% using study reconstruction.

Figure 8b shows the lowest low contrast visibility score is 1.33% for F1-120-80- 10 using IQ-reconstruction. The IQ-reconstruction have a lower score than the S-reconstruction. The F1-120-80-10-S and F1-120-50-10-S have a score of 1.91% and 2.57%, respectively, while its only 2.14% when its F1-120-50-10-IQ. The highest difference between each reconstruction happens in F0-100-10-10, because when it uses IQ-reconstruction the score is only 3.75%, but it is 13.58% when study reconstruction is used.

Figure 9a shows the spatial resolution test. Both F1-120-50-10 and F1-120-80-10 passed the tolerance of 10-line pair (lp)/cm, but when using the study reconstruction, it did not. The F0-100-10-10 only capable of yielding in 8 lp/cm and 5 lp/cm using IQ and S-reconstruction, respectively. 13 and 11 lp/cm from F1-120-50-10-IQ and F1-120-80-10-IQ turned into 6 lp/cm after using the S-reconstruction. **Figure 9b** shows the scale test, in which all protocols passed the tolerance of ± 1 mm. The reconstruction change does not result in any significant changes towards the results.

Discussion

Based on the results, the bowtie filter and higher mAs create a great impact to the mean HU value for acquisition protocol using 100 kVp and 120 kVp. On 100 kVp settings with or without filter, mA higher than 40 mA produce an HU value closer to those in CT image, but on 120 kVp settings, F1 or F0, it only needs to be higher than 20 mA. Both mAs and kVp affect the amount and quality of X-rays that penetrate through the object being scanned. Higher mAs will increase the number of X-rays leading to less noise, while higher kVp would raise the energy of X-rays; thus, they can penetrate deeper into the object being scanned.[11,28] Meanwhile, a bowtie filter can reduce the x-ray scatter that reaches the detector since it affects the beam hardening effect.[8,29] A previous study conducted by Taniguchi[13] in 2021 shows that the mean HU value in CBCT could change using different parameters, similar to what happened in Figure 4.[13] The mean HU value depends on photon energies, and its value tends to be higher in the off-centre position than in the isocentre position, as shown in **Figure 6c**. This study correlates with the results since the 120 kVp using F1 has the most comparable mean HU value.

From **Table 5** to **Table 7**, the use of reconstruction parameters also affects the HU value, affecting the accuracy of dose calculations. The CBCT reconstruction algorithm also works as a scatter correction.[8] S-reconstruction protocols tend to produce the HU values closer to the HU value based on CT Simulator. Despite that, the reconstruction parameters given by XVI (M and H) also generate suitable HU values. For example, the maximum difference using F1-120-50-10-S is 49, which happens in bone 800 mg/cc insert, while using F1-120-50-10-M and F1-120-50-10-H, is 83, which happens in bone 800 mg/cc and lung inhale insert.

It should be noted that S-reconstruction use several different reconstruction parameter values available. Based on the XVI reconstruction guide, the "Interpolation" parameter value in S-reconstruction uses "Bilinear" instead of "Partial2". "Partial2" works by interpolating the projection image by multiplying of two and then does a near-neighbour interpolation along the back projection. "Bilinear" uses four-point (2D) interpolation along the back-projection resulting in better reconstruction than "Partial2" but slower than "Partial2". Another parameter value changed is the "ReconstructionDataType", S-reconstruction use "Float", which means the XVI does a slow reconstruction that develops higher quality compared to "Short". M- and H-reconstruction used "Short". The "PreFilter" parameter value was also changed in S-reconstruction from "None" to "Median5". This value will apply a median window filter on the projection images where the window includes a pixel and the four adjacent pixels. The H- and M-reconstruction use "None", which means XVI does not apply a pre-filter to the projection images, "Median5" contrast is higher than "None", but its resolution is lower than "None". All of the parameter value that was changed above correlate with how the algorithm interpolates the information received by the detectors. The size of detectors, under-sampling of sampling frequency or cone beam divergence could result in the aliasing artefact. Aliasing artefact happens to the nearest volume slice with the source, which collects more rays per voxel. By introducing better interpolation, the aliasing artefact could be avoided.[17] Choosing the proper reconstruction parameters value could increase dose calculation accuracy.

After dose calculation, shown in **Figure 7**, all calculations using F0-100-10-10 only passed the TG 119 dose goal when using F0-100-10-10-M. The F0-100-10-10-S did not pass the dose goal because of dose in D90% PTV didn't reach 5000 cGy and F0-100-10-10-H because the dose in OAR left parotid was too high. What happens in F0-100-10-10-M is related to dose uncertainty.[29] Dose uncertainty could happen when using improper pre-set and is related to image uncertainty inside certain voxel or image uncertainty of the surrounding voxels.[29] Example of image uncertainty happens in F1-100-10-10 calibration curve, shown in **Figure 4**, where the HU value of bone 800 mg/cc is similar to the HU value from the CT image. These uncertainties could also occur because of the image registration process or the limited CBCT FOV size.[29]

All F1-120-50-10 and F1-120-80-10 parameters, for different reconstructions, meet the TG 119 dose goal. However, the F1-120-80-10-M VMAT techniques did not meet the TG 119 dose goal because of the higher dose for OAR left parotid. Despite all that, every calculation yielded in difference not higher than 1%, including those that did not pass the dose goal. Protocols F1-120-80-10-S have the highest dose difference in PTV of 0.13% using IMRT and 0.21% using VMAT. The dose difference in PTV for F1-120-50-10, F1-120-50-10-M, and F1-120-50-10-H is no higher than 0.4%, the highest is 0.3% and 0.37% for VMAT and IMRT for F1-120-50-10-M, respectively. Different reconstruction results in different dose calculations, while the F1-120-50-10 experience a dose difference in PTV of 0.11% and 0.19% for VMAT and IMRT, respectively. Meanwhile, the F1-120-50-10-H are 0.18% and 0.23% for VMAT and IMRT, respectively. Protocols using higher resolution reconstruction have smaller dose differences in PTV. This corresponds with the previous study by Souleyman[18] and Dunlop[30], which indicate a dose difference not higher than 2.5% when using F0-100-10-10 acquisition protocol.[13,18] On average, the highest dose difference in PTV is 0.47% and 0.41%, which happen in F0-100-10-10 using VMAT and F1-120-80-10-M with IMRT.

Friedman statistical tests were used to find the significant dose differences in PTV among $D_{20\%}$, $D_{90\%}$, and $D_{99\%}$ from all of the protocols. Protocols using IMRT and VMAT produce p-value of 0.002 and 0.004, which both are smaller than 0.05. This score indicates that each dose generated has no significant difference from the other. In other words, they are all the same.

For OARs, such as the spinal cord, the maximum dose in F1-120-80-10 shows the highest dose difference of 2.68% and

3.46% since the doses are 3808 cGy and 3694 cGy, for VMAT and IMRT, respectively. The maximum dose for left parotid happens to be 1.14% or 5208 cGy for VMAT using F1-120-50-10 and 2.77% or 5401 cGy for IMRT using F0-100-10-10-H. Meanwhile, for right parotid, the highest dose is 3.77% or 4894 cGy and 1.53% or 5088 cGy for VMAT and IMRT using F0-100-10-10-H. The results agree with a study by Rong[21] from 2010, which shows a dose difference in PTV of no more than 1%, and a high similarity between plans using CBCT and CT simulator images.[13,21] This correlates with the size of the object being scanned while looking for the HU-RED calibration curve, which affects the scatter contamination.[13,21] Scatter contamination is an artefact that is most frequent in his study.[13,21]

In terms of CI, the closer it is to 1 means, the more conformal the dose distribution is. Dose calculation using CT simulator images produces CI of 0.92 and 0.85 for VMAT and IMRT, respectively. The highest CI using CBCT images happen to be 0.93 for F1-120-80-10 using VMAT and 0.86 for F1-120-80-10-M, F1-120-80-10-H, F1-120-50-10-M, F0-100-10-10-M and F0-100-10-10-H using IMRT. For HI, the closer the value to 0 means, the more homogenous the dose distribution. HI using CT simulator images is 0.072 and 0.09 using VMAT and IMRT, respectively. When using CBCT images, the lowest HI is 0.072 for F1-120-80-10 using VMAT and 0.089 for F1-120-80-10 and F0-100-10-10 using IMRT.

Dose distribution is evaluated using Gamma Index (GI) by comparing the 3D dose distribution using Gamma Criteria DD/DTA 2%/2 mm. The lowest result is 97% and 96.8% when comparing F1-100-10-10-H using IMRT and VMAT. F1-120-50-10 have the highest score of 98.5% and 98.3% for IMRT and VMAT. The results match with a study done by Rafic[31] in 2015, having a GI score of 95.88% when comparing planar dose with GI DD/DTA 3%/3 mm. It also matches with other study conducted by Souleyman[18], who obtained 96.4% for sagittal, 95.95% for frontal and 98.6% for transversal.[13,18] This shows that CBCT images can be used for dose calculation, and choosing suitable acquisition and reconstruction parameters is necessary to improve the quality and accuracy of dose calculation using CBCT images. For CBCT XVI, Small mode acquisition using the F1-120-50-10 or F1-120-80-10 yields the best results. For the reconstruction parameters, both XVI reconstruction parameters (M and H) are adequate to be used in clinical cases.

Image quality tests were done using Catphan 503 phantom. The CBCT XVI have its own reconstruction that is used in image quality test (IQ), as explained in **Table 4** and was also used for comparison. Uniformity tests have a tolerance value of 1.5%, as shown in **Figure 8a**. The F1-120-80-10-H and F1-120-80-10-M have lower scores compared to F1-120-80-10-S and F1-120-80-10-IQ. The F1-120-50-10-IQ score is the lowest among his other reconstruction. Meanwhile, a score higher than 3% happens every F0-100-10-10 acquisition. The highest happens in F0-100-10-10-H. This proves that reconstruction also plays a role in image uniformity. Improper image acquisition parameters lead to higher image uncertainty, and it cannot be fixed using better reconstruction.

In the low contrast visibility test, **Figure 8b**, all of the parameters reconstructed using IQ-reconstruction shows lower scores compared to the same image reconstructed with S-, M-, or H-reconstructions. All images reconstructed using M- and H-reconstructions do not pass the tolerance, because their scores are higher than 3%. Again, all F0-100-10-10 acquisitions have higher scores compared to all other parameters. F0-100-10-10-S have the highest score, while the F0-100-10-10-IQ score is the lowest among all of the F0-100-10-10 acquisition protocols. This further proves that reconstruction plays a role in image quality by reducing certain artefacts and scatter contamination. Although, without a suitable image acquisition protocol, proper image quality cannot be achieved depending only on the reconstruction algorithm.

Spatial resolution, **Figure 9a**, every image reconstructed using other than IQ reconstruction does not pass higher than 8 lp/cm. Only F1-120-80-10-IQ and F1-120-50-10-IQ passed the tolerance of 10 lp/cm with scores of 13 lp/cm and 11 lp/cm. This is possible because S-reconstruction parameters use "Median5" algorithm, IQ-reconstruction use "None" algorithm. The difference is, "Median5" generate lower resolution compared to "None", but it develops higher contrast compared to "None".

During the scale test, the results are all still in tolerance of ±1 mm when using XVI and study reconstruction. All of the image quality test results are in accordance with a previous study done by Kamath[11] in 2011, who studied the image quality of CBCT XVI using various mAs.[11,28] This study shows that the higher the mAs, the lower its mean pixel value, which correlates with the decrease of noise and the increase of its Contrast to Noise Ratio (CNR).[11,28] The CBCT bowtie filter (F1) improves the image quality since it can decrease the dynamic range of the detector during a CBCT scan.[8] Uniform flux could reach the detector, reducing the surplus of fluence near the skin zone and absolute scatter signal at the edge zone.[8] The reduction of the absolute scatter signal improves the scatter-to-primary ratio (SPR) behind the centre of the phantom and thus image quality.[8]

Conclusion

This study examined the feasibility of improving the accuracy and quality of dose calculation using CBCT images by finding suitable acquisition and reconstruction parameters. Using different acquisitions and reconstructions could result in more comparable HU-RED calibration curves to ensure a precise result in the dose calculation. The results show that despite using a non-comparable calibration curve, the dose difference is not more than 1%. Nevertheless, acquiring images with suitable acquisition protocols is important because images acquired with unsuitable protocols contain high uncertainty, such as artefacts

and noise. The CBCT reconstruction protocol works as scatter correction and can correct the images obtained. However, it won't fix images acquired using non-adequate protocol. Based on the dosimetry and image quality aspects, it shows that using the F1-120-50-10 acquisition parameters is highly recommended by this study because it generates a high dose accuracy and image quality. The F1-120-50-10 has the highest dose difference of 0.23% using the H-reconstruction and VMAT technique, and the lowest GI score is 97.8% using the M-reconstruction and VMAT technique. Regarding image quality, this protocol has a uniformity test score of 1.21%, low contrast visibility test of 2.14%, and a spatial and resolution test of 11 lp/cm. This protocol is the most optimal image and should be used clinically.

This study was limited to the imaging parameter in a small mode field of view available on CBCT XVI (Elekta Oncology Systems, UK), mainly used for head and neck (HN) radiation treatment small mode for head and neck only. Further study can explore another mode of FOV (for different anatomical locations), such as Medium and Large.

Acknowledgement

The authors thank the management and all staff members in the Department of Radiotherapy, dr. Cipto Mangunkusumo General Hospital. This study is partially funded by Research Grant Universitas Indonesia with contract number NKB-1139/UN2.RST/HKP.05.00/2022.

References

1. Castadot P, Lee JA, Geets X, Grégoire V. Adaptive Radiotherapy of Head and Neck Cancer. Semin Radiat Oncol. 2010;20(2):84-93. https://doi.org/10.1016/j.semradonc.2009.11.002
2. de Smet M, Schuring D, Nijsten S, Verhaegen F. Accuracy of dose calculations on kV cone beam CT images of lung cancer patients. Med Phys. 2016;43(11):5934-5940. https://doi.org/10.1118/1.4964455
3. Kataria T, Gupta D, Bisht SS, et al. Adaptive radiotherapy in lung cancer: Dosimetric benefits and clinical outcome. British Journal of Radiology. 2014;87(1038). https://doi.org/10.1259/bjr.20130643
4. Scarfe WC, Farman AG. What is Cone-Beam CT and How Does it Work? Dent Clin North Am. 2008;52(4):707-730. https://doi.org/10.1016/j.cden.2008.05.005
5. Veiga C, McClelland J, Moinuddin S, et al. Toward adaptive radiotherapy for head and neck patients: Feasibility study on using CT-to-CBCT deformable registration for "dose of the day" calculations. Med Phys. 2014;41(3). https://doi.org/10.1118/1.4864240
6. Ding GX, Duggan DM, Coffey CW, et al. A study on adaptive IMRT treatment planning using kV cone-beam CT. Radiotherapy and Oncology. 2007;85(1):116-125. https://doi.org/10.1016/j.radonc.2007.06.015
7. Abe T, Tateoka K, Saito Y, et al. Method for Converting Cone-Beam CT Values into Hounsfield Units for Radiation Treatment Planning. Int J Med Phys Clin Eng Radiat Oncol. 2017;6(4):361-375. https://doi.org/10.4236/ijmpcero.2017.64032
8. Mail N, Moseley DJ, Siewerdsen JH, Jaffray DA. The influence of bowtie filtration on cone-beam CT image quality. Med Phys. 2009;36(1):22-32. https://doi.org/10.1118/1.3017470
9. Pauwels R, Jacobs R, Singer SR, Mupparapu M. CBCT-based bone quality assessment: Are Hounsfield units applicable? Dentomaxillofacial Radiology. 2015;44(1). https://doi.org/10.1259/dmfr.20140238
10. Schneider U, Pedroni E, Lomax A. The Calibration of CT Hounsfield Units for Radiotherapy Treatment Planning. Phys Med Biol. 1996;41(1):111. http://iopscience.iop.org/0031-9155/41/1/009
11. Kamath S, Song W, Chvetsov A, et al. An Image Quality Comparison Study between XVI and OBI CBCT Systems. J Appl Clin Med Phys. 2011;12(2):3435; 2011. https://doi.org/10.1120/jacmp.v12i2.3435
12. Song WY, Kamath S, Ozawa S, et al. A dose comparison study between XVI® and OBI® CBCT systems. Med Phys. 2008;35(2):480-486. https://doi.org/10.1118/1.2825619
13. Taniguchi T, Hara T, Shimozato T, et al. Effect of computed tomography value error on dose calculation in adaptive radiotherapy with Elekta X-ray volume imaging cone beam computed tomography. J Appl Clin Med Phys. 2021;22(9):271-279. https://doi.org/10.1002/acm2.13384
14. Jaffray DA, Siewerdsen JH, Wong JW, Martinez AA. Flat-panel cone-beam computed tomography for image-guided radiation therapy. International Journal of Radiation Oncology*Biology*Physics. 2002;53(5):1337-1349. https://doi.org/10.1016/S0360-3016(02)02884-5
15. Hyer DE, Serago CF, Kim S, Li JG, Hintenlang DE. An organ and effective dose study of XVI and OBI cone-beam CT systems. J Appl Clin Med Phys. 2010;11(2):181-197. https://doi.org/10.1120/jacmp.v11i2.3183
16. Oborska-Kumaszyńska D, Northover D. EP-1723: Optimisation of an Elekta XVI (R.5.0.2) system for clinical protocols – image quality vs dose. Radiotherapy and Oncology. 2017;123. https://doi.org/10.1016/S0167-8140(17)32255-7

17. Schulze R, Heil U, Groß D, et al. Artefacts in CBCT: A review. Dentomaxillofacial Radiology. 2011;40(5):265-273. https://doi.org/10.1259/dmfr/30642039
18. Souleyman S, Maria K, Cheikh T, Karima KK. Impact of acquisition protocols on accuracy of dose calculation based on xvi cone beam computed tomography. J Med Phys. 2021;46(2):94-104. https://doi.org/10.4103/jmp.JMP_128_20
19. Little DP. Image quality improvement for medium and large field of view Elekta XVI scans. Australas Phys Eng Sci Med. 2019;42(4):1153-1164. https://doi.org/10.1007/s13246-019-00817-7
20. Srnivasan K, Mohammadi M, Shepherd J. Applications of linac-mounted kilovoltage Cone-beam Computed Tomography in modern radiation therapy: A review. Pol J Radiol. 2014;79:181-193. https://doi.org/10.12659/PJR.890745
21. Rong Y, Smilowitz J, Tewatia D, Tomé WA, Paliwal B. Dose Calculation on KV Cone Beam CT Images: An Investigation of the Hu-Density Conversion Stability and Dose Accuracy Using the Site-Specific Calibration. Medical Dosimetry. 2010;35(3):195-207. https://doi.org/10.1016/j.meddos.2009.06.001
22. Hansen MS, Kellman P. Image reconstruction: An overview for clinicians. Journal of Magnetic Resonance Imaging. 2015;41(3):573-585. https://doi.org/10.1002/jmri.24687
23. Rached PA, Lio J, Canola C, et al. Computed Tomographic-Dacryocystography (CT-DCG) of the Normal Canine Nasolacrimal Drainage System with Three-Dimensional Reconstruction. Vet Ophthalmol. 2011;14(3):174-9. https://doi.org/10.1111/j.1463-5224.2010.00861.x
24. Ezzell GA, Burmeister JW, Dogan N, et al. IMRT commissioning: Multiple institution planning and dosimetry comparisons, a report from AAPM Task Group 119. Med Phys. 2009;36(11):5359-5373. https://doi.org/10.1118/1.3238104
25. Sarria GR, Schmitt H, Jahnke L, et al. Cone Beam CT-Based Daily Adaptive Planning or Defined-Filling Protocol for Neoadjuvant Gastric Cancer Radiation Therapy: A Comparison. Adv Radiat Oncol. 2021;6(1). https://doi.org/10.1016/j.adro.2020.09.026
26. Mynampati DK, Yaparpalvi R, Hong L, Kuo HC, Mah D. Application of AAPM TG 119 to volumetric arc: Therapy (VMAT). J Appl Clin Med Phys. 2012;13(5):108-116. https://doi.org/10.1120/jacmp.v13i5.3382
27. ICRU Report 62: Prescribing, Recording and Reporting Photon Beam Therapy. Published online November 1, 1999.
28. Cozzi L, Fogliata A, Buffa F, Bieri S. Dosimetric impact of computed tomography calibration on a commercial treatment planning system for external radiation therapy. Radiotherapy and Oncology. 1998;48(3):335-338. https://doi.org/10.1016/S0167-8140(98)00072-3
29. Barateau A, de Crevoisier R, Largent A, et al. Comparison of CBCT-based dose calculation methods in head and neck cancer radiotherapy: from Hounsfield unit to density calibration curve to deep learning. Med Phys. 2020;47(10):4683-4693. https://doi.org/10.1002/mp.14387
30. Dunlop A, McQuaid D, Nill S, et al. Vergleich unterschiedlicher CT-Kalibrierungsmethoden zur Dosisberechnung auf Basis der Kegelstrahlcomputertomographie. Strahlentherapie und Onkologie. 2015;191(12):970-978. https://doi.org/10.1007/s00066-015-0890-7
31. Rafic M, Ravindran P. Evaluation of on-board imager cone beam CT hounsfield units for treatment planning using rigid image registration. J Cancer Res Ther. 2015;11(4):690-696. https://doi.org/10.4103/0973-1482.146087